

N73-28593

IFSM-73-42

TO ELECTRONIC  
D-FOSDZ MECHANICS

# LEHIGH UNIVERSITY



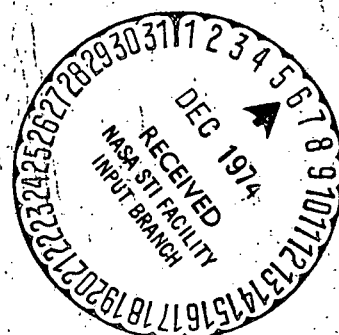
THE INTERACTION BETWEEN INCLUSIONS AND CRACKS

## CASE FILE COPY

By

F. ERDOGAN

TECHNICAL REPORT NASA TR-73-12



MAY 1973

NATIONAL AERONAUTICS AND SPACE ADMINISTRATION  
GRANT NGR-39-007-011

## THE INTERACTION BETWEEN INCLUSIONS AND CRACKS

F. Erdogan

Lehigh University, Bethlehem, Pennsylvania

### 1. INTRODUCTION

The fracture strength of composite materials in general and ceramics in particular depends to a considerable extent on the size, shape, orientation, and distribution of flaws or imperfections in the material. In studying the "bulk strength" and other bulk properties of the composite it is generally assumed that these flaws are randomly distributed throughout the material and hence the medium is statistically homogeneous. Therefore, in this type of studies the very nature of the phenomenon requires that some kind of a statistical strength theory be used as a guide in the investigations.

In a second type of approach to fracture studies, one is basically interested in the more detailed treatment of the fracture initiation phenomenon in the localized regions. In such an approach it is generally conjectured that the macroscopic fracture of the medium will initiate at and will propagate from a "dominant flaw". This is usually the flaw which has, from the viewpoint of the fracture resistance of the material, the worst possible combination of size, shape, orientation, and location in the structural part which has a given overall geometry and is subjected to a given system of external loads and environmental conditions. The dominant flaw may be caused by residual stresses or by some other type of loading before the part is put into use, it may be a manufacturing flaw (such as entrapped gas, weak impurities, imperfect bonding, and the

geometric singularities arising from the particular shape of the constituent materials), or it may result from the growth of a "microflaw" due to the cyclic nature of the operating stresses. In some cases it may be possible to detect such flaws by using nondestructive testing techniques. However, more often, in studies relating to structural integrity and reliability one simply assumes their existence.

In ceramics one may assume that the composite medium consists of the matrix, the inclusions with elastic properties different than that of the matrix, and the pores. Generally, from the viewpoint of the fracture strength, the worst imperfections are the cracks in the matrix and/or in the inclusions. Thus, in the most elementary sense the main objective of fracture studies in ceramics is to develop a technique for the solution of the following mechanics problem: To find the magnitude of the external loads which can be carried safely by a structural part with given matrix-dominant crack-inclusion-pore geometry under given environmental conditions. It is clear that the problem has three different aspects which may be studied more or less independently:

(a) Determination of the "characteristic strength parameter" of the material. This is the experimental work aimed at determining the inherent resistance of the constituent materials to fracture corresponding to the conjectured mode of failure, such as "brittle" or "quasi-brittle" (i.e., low energy-type) fracture, "ductile" (i.e., high energy-type) fracture, shear or tensile cleavage, and debonding or delamination. Example: fracture toughness,  $G_{IC}$ .

(b) The solution of the mechanics problem for the given geometry and the external loads in order to determine the "critical load factor" representing the severity of the applied loads and corresponding to the conjectured mode of fracture. Example: strain energy release rate,  $G_I$ .

(c) Development of an appropriate fracture theory and a related quantitative "fracture criterion". This is usually nothing but the direct comparison of the "characteristic strength parameter" of the material with the "critical load factor". Example:  $G_I \leq G_{IC}$ . It is clear that in fracture studies the development of the fracture theory and selection of a proper fracture criterion must precede the experimental determination of

the characteristic strength parameters and the theoretical evaluation of the corresponding critical load factors.

In this paper after a brief review of some of the current fracture theories, a group of mechanics problems of practical interest relating to the elastic interaction between cracks and inclusions will be identified and a summary of the results will be presented.

## 2. FRACTURE THEORIES

Due to the lack of full physical understanding of the fracture phenomenon in solids and the lack of sufficiently powerful mathematical tools, at the present time there is no consistent theory dealing with all the relevant aspects of the phenomenon. Partly for this reason and partly because of the divergence in the background and interest of the researchers studying the field, generally the existing theories treat the subject from only one of the three points of view, namely (a) atomic (or microscopic), (b) microstructural, and (c) continuum. From the viewpoint of structural applications the theories which provide the quantitative tools to deal with the problem are mostly the continuum theories which are based on the notions and principles of the classical thermodynamics and the continuum solid mechanics. Hence, the discussion given in this section will include only these theories.

### (a) Energy Balance Theories

The fracture theories which are based on the energy balance follow directly from the thermodynamic principle which states that in a given continuum

$$\dot{U} = \dot{T} + \dot{V} + \dot{D} , \quad (1)$$

where  $U$  is the work done by the external loads,  $T$  is the kinetic energy,  $V$  is the (recoverable) potential energy,  $D$  is the total dissipation, and the dot stands for the time rate of change [1]. (1) is valid for the whole as well as a toroidal portion of the body enclosing the leading edge or the periphery of the crack. At the onset of (quasi-static) crack propagation in ideally brittle materials (1) is easily shown to reduce to the Griffith criterion, namely

$$G_I = G_{IC} = 2\gamma_S, \quad (2)$$

where  $G_I$  is the "strain energy release rate" or the "crack extension force" per unit length of the crack front, and  $\gamma_S$  is the specific surface tension energy. In the extension of the theory to quasi-brittle type fracture [2,3]  $G_{IC}$  is interpreted as the "fracture toughness" of the material, or  $\gamma_S$  is replaced by  $\gamma_F$ , the "fracture energy" (i.e., the amount of energy required to create a unit area of fracture surface). In either case, noting that  $G_I = (1-\nu^2)K_I^2/E$ , the criterion may also be stated in terms of the "stress intensity factor" as follows:

$$K_I = K_{IC} \quad (3)$$

where  $K_I$  is the stress intensity factor (for example  $K_I = k_I\sqrt{\pi} = \sigma_0\sqrt{\pi a}$  for an infinite solid with a through crack of length  $2a$  and subjected to a uniform stress perpendicular to the plane of the crack), and  $K_{IC}$  is assumed to be a material constant.

Even though the underlying principle of the theory is quite general, quantitatively it gives good results only for "plane strain" type of configurations where the characteristic size of the "dissipation zone" surrounding the leading edge of the crack is small in comparison with the characteristic crack size. Thus, the subscript I in (2) and (3) is usually meant to stand for "plane strain". In the general case writing [2,3]  $G = G_C$ , one may interpret the load factor  $G$  as the "energy available" (through external addition or internal release) for fracture, and the characteristic strength parameter  $G_C$  as the "energy required for the creation of unit fracture area". In practice the difficulty lies in evaluating  $G$  with sufficient accuracy and in properly isolating and measuring  $G_C$ . The present chaotic state of characterization of the so-called "plane stress fracture" is a good example. Even though developed only for nonlinear elastic (hence, nondissipative) solids, recent attempts of computing  $G$  through path-independent integrals (known as the J-integral) have met with partial success [4-6]. However, the problem of a reliable characterization for  $G_C$  still remains very elusive.\* It should be noted that

\*The recent investigations on the development of the "crack extension resistance curve" for (or the so-called  $K_R$ -characterization of) the fracture of sheet materials appear to be promising. However, in this case too the isolation of a geometry-independent characteristic strength parameter has not yet been successful.

regardless of the generality of its underlying principle, as it is understood and applied in practice, a tacit requirement of the energy balance theory is that the stress and deformation fields remain "self-similar" as the crack propagates, which in a narrow sense means that the crack remains in its own plane as it propagates, the crack front advancing in an autonomous fashion. This is the case only if (a) the crack remains imbedded in the same homogeneous medium as it propagates, i.e., it does not intersect any phase boundary or bi-material interface, and (b) the crack is and remains as an interface crack. For example if  $k_1$  and  $k_2$  are the in-plane tensile and shear components of the stress intensity factor\* at the tip of a crack lying along the interface of two elastic materials with constants  $\mu_1, \kappa_1$  and  $\mu_2, \kappa_2$  ( $\mu_i$ : shear modulus,  $\kappa_i = 3-4\nu_i$  for plane strain,  $\kappa_i = (3-\nu_i)/(1+\nu_i)$  for plane stress,  $\nu_i$ : Poisson's ratio), the (elastic) strain energy release rate (per unit crack extension/per unit crack front) is given by [7]

$$G = \left( \frac{\partial U}{\partial a} \right)_{12} = \frac{\pi}{4} \frac{(\mu_1 + \kappa_1 \mu_2)(\mu_2 + \kappa_2 \mu_1)}{\mu_1 \mu_2 [(1+\kappa_1)\mu_2 + (1+\kappa_2)\mu_1]} (k_1^2 + k_2^2), \quad (4)$$

which, for homogeneous materials reduces to

$$G = \frac{\partial U}{\partial a} = \frac{\pi(1+\kappa)}{8\mu} (k_1^2 + k_2^2). \quad (5)$$

In (4) and (5), again the assumption is that the crack remains in its own plane as it propagates. In applying (4) the related characteristic strength parameter,  $(G_C)_{12}$  will be the fracture energy of the particular adhesion.

#### (b) C.O.D.-Characterization

Contending that fracture is basically creation of new surfaces in the solid resulting from rupture-separation of the material around the leading edge of the crack, particularly in the presence of large scale inelastic deformations, some investigators have concentrated their attention at the crack tip region and proposed the argument that a true measure of the severity

---

\*In this paper the definition of the stress intensity factors  $k_1, k_2, k_3$  does not include  $\sqrt{\pi}$  and is based on the asymptotic relations of the form  $\sigma_{\theta\theta}(r, 0) \approx k_1/\sqrt{2r}$ ,  $\sigma_{r\theta}(r, 0) \approx k_2/\sqrt{2r}$ ,  $\sigma_{\theta z}(r, 0) \approx k_3/\sqrt{2r}$  for small  $r$ ,  $r$  and  $\theta$  being the polar coordinates at the crack tip.

of the external loads may be the deformation state at the crack tip characterized by the amount of stretch ( $\delta$  or C.O.D., the proposed load factor) suffered by a thin layer of material in the plane and ahead of the crack. In turn the fracture resistance of the material may be characterized by the value of this stretch at rupture ( $\delta_C$ , the proposed strength parameter) which is conjectured to be (with certain qualifications) a material constant [8-11]. The criterion (which has been standardized in the United Kingdom and has found so far a wider acceptability in Europe than in the U.S.) appears to work rather successfully for "plane stress" type fracture of thin sheets with relatively large plastic zones around the crack. The application of this criterion too requires that the extension of the crack be co-planar with the crack and the crack remain imbedded in the same homogeneous medium.

#### (c) Critical Stress Criterion

In ceramics and other composites, because of the nonhomogeneous nature of the medium, usually the stress state around the leading edge of the crack is of the mixed-mode type, and one occasionally encounters the problem of a crack intersecting a bi-material interface. In cases such as these either the crack may not remain co-planar or the stress and displacement fields around the crack tip may not remain self-similar as the crack propagates.\* Thus, in this type of fracture studies the fracture theories and criteria based on the notions of energy balance or critical crack opening stretch mentioned above will be either ineffective or inapplicable, and clearly a more flexible approach is needed. For brittle and most quasi-brittle materials the "maximum cleavage stress" criterion discussed in [13] or some variation of it may provide an acceptable and a very simple working tool. The modification of the criterion is necessary primarily to be able to deal with problems in which instead of the standard  $r^{-1/2}$  singularity the stresses have either oscillating and/or arbitrary power singularity (i.e.,  $r^{-\alpha}$ ,  $0 < \text{Re}(\alpha) < 1$ ), as in the case of cracks lying on or intersecting the interfaces. The

---

\*As will be pointed out later in this paper for a crack tip terminating at an interface the power of the singularity is no longer  $-1/2$  and the  $r, \theta$ -dependence of the stresses is completely different than that of a crack tip imbedded in a homogeneous medium (see [12]).

argument here is as follows:

Due to the very high concentration of stresses and strains and to highly nonlinear and inelastic nature of the phenomenon, even in brittle materials, the response of the medium in a small toroidal region enclosing the leading edge of the crack cannot be accurately obtained. Noting that the initial radius of curvature of the crack surface at the tip region may be as small as the inter-atomic distances, even if the necessary mathematics were available, there is always a region in which the continuum theories of solids will be inapplicable. Let  $\delta_p$  be the radius of the cross section of this region (measured from the edge of the crack).  $\delta_p$ , called the "characteristic process zone size", may depend on the microstructure and continuum properties of the material as well as on the environmental conditions. Even though what goes on in this region (as far as the material response is concerned) is very important and may affect the response outside the region, it cannot quantitatively be incorporated into a continuum model. Hence any continuum theory or criterion will have to be based on the quantities which can be calculated and measured outside this region. Thus, we are essentially forced to ignore the toroidal region ( $r < \delta_p$ ,  $-\pi < \theta < \pi$ ), where  $r$  and  $\theta$  are the polar coordinates at the crack tip in the plane perpendicular to the crack front. The "critical stress" criterion may then be stated as

the fracture propagation will take place in the direction  $\theta = \theta_C$  for which the cleavage stress  $\sigma_{\theta\theta}(\delta_p, \theta_C)$  is maximum and when

$$\sigma_{\theta\theta}(\delta_p, \theta_C) = \sigma_C, \quad (6)$$

where  $\sigma_C$  is constant for a given material under given environmental conditions.

(6) is valid if the "weak link" is a particular homogeneous medium surrounding the crack tip. However if the singular point is at a bi-material interface and if the weak link is the adhesion along the interface, then (6) may be modified as

$$(\sigma_C)_{12} = \begin{cases} (\sigma_{\theta\theta}^2 + \sigma_{r\theta}^2)^{1/2}, & \sigma_{\theta\theta} > 0, \\ \sigma_{r\theta} + f\sigma_{\theta\theta} & , \quad \sigma_{\theta\theta} < 0, \end{cases} \quad (r = (\delta_p)_{12}, \theta = \theta_{12}) \quad (7)$$

where  $(\sigma_C)_{12}$  represents the adhesive strength of and  $(\delta_p)_{12}$  is the characteristic process zone size for the

given bi-material interface, and  $\theta_{12}$  is the radial direction along the interface. In (7) for  $\sigma_{\theta\theta} > 0$  the right-hand side represents the magnitude of the (tensile) stress vector acting on the surface of adhesion. For  $\sigma_{\theta\theta} < 0$  the mode of adhesive rupture has to be shear, and the shear stress  $\sigma_{r\theta}$  will be reduced somewhat by "friction". The term  $f\sigma_{\theta\theta}$  is therefore added to  $\sigma_{r\theta}$  to account for this effect. Finally, in order to be able to apply the criterion in practical problems, it will be assumed that due to relative "smallness" of  $\delta_p$

the effect of the phenomena taking place within the process zone  $r < \delta_p$  on the stresses outside this region is negligible.

Thus, for example, on a crack front imbedded in a homogeneous brittle medium, if  $k_1$  and  $k_2$  are the tensile and shear components of the stress intensity factor in a plane perpendicular to the leading edge of the crack, we have [13]

$$\sigma_{\theta\theta}(\delta_p, \theta) \approx \frac{1}{\sqrt{2\delta_p}} \cos \frac{\theta}{2} \left( k_1 \cos^2 \frac{\theta}{2} - \frac{3}{2} k_2 \sin \frac{\theta}{2} \right), \quad (8)$$

and  $\theta_C$  is obtained from  $(\partial\sigma_{\theta\theta}/\partial\theta) = 0$ ,  $(\partial^2\sigma_{\theta\theta}/\partial\theta^2) < 0$ , or

$$k_2(1 - 3\cos\theta_C) - k_1\sin\theta_C = 0,$$

$$3k_2\sin\theta_C - k_1\cos\theta_C < 0. \quad (9.a,b)$$

For a crack terminating at or intersecting the interface the stresses around the singular point at the interface are of form (for details see [12] and [14])

$$\sigma_{ij}(r, \theta) \approx \frac{1}{r^\alpha} [k_1 f_{1ij}(\theta) + k_2 f_{2ij}(\theta)],$$

$$(i, j = r, \theta; \quad 0 < \text{Re}(\alpha) < 1; \quad -\pi < \theta < \pi). \quad (10)$$

It is seen that unlike the energy balance and the critical C.O.D. criteria, the criterion given by (6) or (7) can be applied to fracture problems represented by (8) or (10) with equal facility. It should be pointed out that for symmetrically loaded (i.e.,  $k_2 = 0$ ) homogeneous materials, in the absence of large scale inelastic deformations around the crack front, all three theories described in this section are equivalent and would give the same results.

### 3. INTERACTION BETWEEN INCLUSION AND CRACKS

Assuming that we have an acceptable "fracture criterion" (e.g., any one of the three criteria discussed in the previous section or some other criterion) and could perform the idealized experiments to determine the related "characteristic strength parameters", the problem is then reduced to the evaluation of the "critical load factor" for the particular structural part with given matrix-crack-inclusion-pore geometry and subjected to a given set of external loads and environmental conditions. The exact treatment of the three-dimensional problem with a regular or a random array of inclusions imbedded into a matrix containing a (dominant) internal crack is hopelessly complicated. Therefore, we will first assume that the composite medium is basically linearly elastic and the effect of the small process or the damage zone around the crack on the stress distribution is negligible. Hence, in the application of any of the fracture criteria, to evaluate the related "critical load factor" it is sufficient to calculate the stress intensity factors  $k_1$  and  $k_2$ , the power of the singularity  $\alpha$ , and the functions  $f_{kij}$ , ( $k, i, j = 1, 2$ ) shown in (8) and (10). The remaining assumptions which are made in this paper concern the idealization of the geometry of the medium in order to make the analysis tractable.

First it will be assumed that the medium is a large composite "plate" or "cylinder" which is under either in-plane stress state or anti-plane shear. It will then be assumed that the elastic matrix contains only sparsely distributed inclusions, which are circular. Hence the mechanical interaction will be primarily between an isolated inclusion (or a hole) and line crack(s) located in the matrix and/or in the inclusion. As in many problems in linear fracture mechanics, the solution of this problem too may be obtained through superposition of two solutions: that of the uncracked medium under a given set of external loads, and that of the cracked medium (i.e., the perturbed solution) in which the crack surface tractions obtained from the previous solution are the only external loads. Clearly, only the second solution has the singular stresses. Special cases of this problem were considered in [15-17]. The results given in this paper are taken from [18-20].

### (a) Symmetrically Loaded Radial Cracks

The problem is described in Figure 1. All the problems which are discussed in this paper may be formulated in terms of a system of singular integral equations of the following form:

$$\begin{aligned} \int_{a_1}^{b_1} \frac{f_1(t)}{t-x} dt + \int_{a_1}^{b_1} k_{11}(x,t) f_1(t) dt + \int_{a_2}^{b_2} k_{12}(x,t) f_2(t) dt \\ = \frac{\pi(1+\kappa_1)}{2\mu_1} p_1(x), \quad (a_1 < x < b_1), \\ \int_{a_2}^{b_2} \frac{f_2(t)}{t-x} dt + \int_{a_1}^{b_1} k_{21}(x,t) f_1(t) dt + \int_{a_2}^{b_2} k_{22}(x,t) f_2(t) dt \\ = \frac{\pi(1+\kappa_2)}{2\mu_2} p_2(x), \quad (a_2 < x < b_2), \quad (11) \end{aligned}$$

where  $p_1$  and  $p_2$  are the known crack surface tractions,  $k_{ij}(x,t)$ , ( $i,j=1,2$ ) are known functions (bounded if the cracks are fully imbedded in a homogeneous medium, of the generalized Cauchy type if one or both cracks intersect the interface), and the unknown density functions  $f_1$  and  $f_2$  are the derivatives of the crack surface displacements (for complete details and the solution see [18-20]).

Even though the formulation is quite general, the numerical results are given for only two typical and somewhat extreme cases, namely the case of a pore (i.e.,  $\mu_2=0$ ) and a hard inclusion with  $(\mu_2/\mu_1)=23$ ,  $\nu_1=0.35$ ,  $\nu_2=0.3$ , which approximately corresponds to a metallic inclusion in an epoxy-type matrix. Table 1 shows the stress intensity factors for a crack in the matrix (i.e.,  $a_2=b_2$ ,  $R < a_1 < b_1$ , Figure 1) under uniaxial stress  $\sigma_0$  at infinity.  $k_{1j}$ , ( $j=1,2$ ) shown in the table are the dimensionless quantities given by

$$k_{11} = \frac{k_1(b_1)}{\sigma_0 \sqrt{c_1}}, \quad k_{12} = \frac{k_1(a_1)}{\sigma_0 \sqrt{c_1}}, \quad (12)$$

where  $2c_1$  is the crack length. Note that in the case of a hole as  $a_1 \rightarrow R$ ,  $k_{12} \rightarrow \infty$ . In the inclusion case the

Table 1. The stress intensity factors for a symmetrically located radial crack ( $c_2 = 0$ ,  $R/c_1 = 2$ ,  $\kappa_1 = 1.6$ ,  $\kappa_2 = 1.8$ ).

	$\mu_2 = 0$		$\mu_2 = 23\mu_1$	
$b/c_1$	$k_{11}$	$k_{12}$	$k_{11}$	$k_{12}$
3.0		$\rightarrow \infty$		$\rightarrow 0$
3.2	1.417	2.274	0.827	0.467
3.5	1.290	1.722	0.874	0.671
4	1.188	1.394	0.918	0.821
5	1.102	1.174	0.957	0.924
6	1.065	1.099	0.973	0.959
8	1.033	1.045	0.987	0.982
$\infty$	1.0	1.0	1.0	1.0

stress intensity factor ratios decrease as the crack approaches the interface, and for  $a_1 = R$  the power of the singularity becomes  $\alpha$  where  $\alpha = 1/2$  for homogeneous material  $0 < \alpha < 1/2$ , for  $\mu_2 > \mu_1$ , and  $1/2 < \alpha < 1$  for  $\mu_2 < \mu_1$  [12]. In the present case (i.e.,  $\mu_2 = 23\mu_1$ ,  $\kappa_1 = 1.6$ ,  $\kappa_2 = 1.8$ ),  $\alpha$  is found to be

$$\begin{aligned}\alpha &= 0.33811, & \text{for plane strain,} \\ \alpha &= 0.28901, & \text{for plane stress.}\end{aligned}\tag{13}$$

In this case the stress intensity factor at  $a_1 = R$  is defined by and found to be

$$k_1(a_1) = \lim_{x \rightarrow a_1} \sqrt{2} (a_1 - x)^\alpha \sigma_{2yy}(x, 0) = 1.375 \sigma_0 c_1^\alpha, \tag{14}$$

where the subscripts 1 and 2 refer to the matrix and the inclusion, respectively. The functions of  $\theta$  giving the angular distribution of the stresses around  $x = a_1 = R$  may be found in [12]. For the crack terminating at the interface, the effect of the modulus ratio  $\mu_2/\mu_1$  on  $\alpha$  and  $k(a_1)$  is shown in Table 2. Table 3 shows the effect of the modulus ratio and the Poisson's ratios on the stress intensity factor in a completely cracked inclusion (i.e.,  $a_2 = -R$ ,  $b_2 = R$ ,  $a_1 = b_1$ ) where

$$k(R) = \lim_{x \rightarrow R} \sqrt{2} (x - R)^\alpha \sigma_{1yy}(x, 0) = k' \sigma_0 R^\alpha. \tag{15}$$

Table 2. The effect of modulus ratio on the stress intensity factors for a crack terminating at the interface ( $a_1 = R$ ,  $b_1/R = 2$ ,  $\kappa_1 = \kappa_2 = 1.8$ ,  $c_1 = (b_1 - a_1)/2$ ).

$m = \frac{\mu_2}{\mu_1}$	$\alpha$	$\frac{k(b_1)}{\sigma_0 \sqrt{c_1}}$	$\frac{k(R)}{\sigma_0 c_1^\alpha}$
0		2.808	
0.05	0.81730	1.615	1.053
1/3	0.62049	1.229	0.5836
1.0	0.5	1.000	1.000
3.0	0.40074	0.8610	1.299
10.0	0.33277	0.7969	1.389
23.0	0.30959	0.7796	1.375
100	0.29387	0.7691	1.345
300	0.28883	0.7667	1.348

Table 3. Stress intensity factor for a completely cracked inclusion ( $a_1 = b_1$ ,  $a_2 = -R$ ,  $b_2 = R$ ,  $k' = k(R)/(\sigma_0 R^\alpha)$ ).

$\frac{\mu_2}{\mu_1}$	$\kappa_1 = \kappa_2 = 1.8$		$\kappa_1 = 2.2, \kappa_2 = 1.8$		$\kappa_1 = 1.8, \kappa_2 = 2.2$		$\kappa_1 = \kappa_2 = 2.2$	
	$\alpha$	$k'$	$\alpha$	$k'$	$\alpha$	$k'$	$\alpha$	$k'$
0.2	0.3662	0.789	0.3809	0.785	0.3203	1.046	0.3385	1.010
0.6	0.4503	1.014	0.4703	0.946	0.4212	1.174	0.4447	1.068
1.0	0.5	1.0	0.5199	0.921	0.4772	1.107	0.5	1.0
2.0	0.5745	0.884	0.5919	0.817	0.5569	0.947	0.5762	0.861
5.0	0.6789	0.656	0.6912	0.619	0.6638	0.694	0.6773	0.650

Table 4 shows the result for a crack intersecting the interface. Here note that there are three singular points and the stress intensity factors  $k_y$  and  $k_{xy}$  at the singular point  $x = R$  are defined by

$$k_y(R) = \lim_{y \rightarrow 0} y^\alpha \sigma_{1yy}(R, y), \quad k_{xy}(R) = \lim_{y \rightarrow 0} y^\alpha \sigma_{1xy}(R, y), \quad (16)$$

and  $2c$  is the total crack length. Further results and examples showing the crack surface displacements may be found in [18].

Table 4. The stress intensity factors for a crack crossing the interface ( $\kappa_1 = 1.6$ ,  $\kappa_2 = 1.8$ ,  $\mu_2/\mu_1 = 23.077$ ,  $\alpha = 0.27326$ ,  $c = (b_1 - a_2)/2$ ).

$\frac{a_2}{R}$	$\frac{b_1}{R}$	$\frac{k(b_1)}{\sigma_o \sqrt{c}}$	$\frac{k(a_2)}{\sigma_o \sqrt{c}}$	$\frac{k_y(R)}{\sigma_o c^\alpha}$	$\frac{k_{xy}(R)}{\sigma_o c^\alpha}$
0	1.0	$\rightarrow \infty$		$\rightarrow -\infty$	$\rightarrow \infty$
0	1.1	0.548	3.564	-0.847	0.170
0	1.3	0.513	3.701	-0.446	0.0894
0	1.5	0.570	3.756	-0.222	0.0565
0	1.7	0.626	3.799	-0.171	0.0342
0	1.9	0.672	3.838	-0.0835	0.0167
0	2.1	0.710	3.874	-0.0113	0.00227
0	2.5	0.765	3.935	0.105	-0.0211
0	3.0	0.811	3.996	0.219	-0.0440
-1.0	1.5		$\rightarrow \infty$	$\rightarrow -\infty$	$\rightarrow \infty$
-0.9	1.5	0.920	5.600	-1.102	0.221
-0.7	1.5	0.954	5.242	-0.954	0.191
-0.5	1.5	0.757	5.003	-0.753	0.151
-0.3	1.5	0.670	4.570	-0.547	0.110
-0.1	1.5	0.598	4.034	-0.363	0.0727
0.1	1.5	0.547	3.481	-0.209	0.0420
0.3	1.5	0.518	2.956	-0.0852	0.0171
0.5	1.5	0.510	2.465	0.0171	-0.00343
0.7	1.5	0.525	1.981	0.108	-0.0216
0.9	1.5	0.572	1.383	0.212	-0.0426
1.0	1.5		$\rightarrow 0$	$\rightarrow \infty$	$\rightarrow -\infty$
0.1	1.1	0.487	3.377	-0.730	0.146
0.3	1.3	0.425	2.978	-0.229	0.0459
0.7	1.7	0.619	1.961	0.211	-0.0424
0.9	1.9	0.731	1.401	0.412	-0.0826
1.0	2.0		$\rightarrow 0$	$\rightarrow \infty$	$\rightarrow -\infty$

(b) Plane Problem for Arbitrarily Located Crack

The results for the general problem of an arbitrarily located crack in a matrix containing an inclusion or a hole are shown in Tables 5-9. Table 5 shows the results for the case in which the crack and the inclusion are symmetrically located with respect to the y-axis (i.e., for  $b=0$ ). Here  $c$  is the distance of the crack

Table 5. Stress intensity factors for a symmetrically located "tangential crack" perpendicular to the load ( $b=0$ ,  $R=2a$ ,  $\kappa_1=1.6$ ,  $\kappa_2=1.8$ ).

	$\mu_2/\mu_1 = 0$		$\mu_2/\mu_1 = 23$	
c/a	$k_{11}=k_{12}$	$k_{21}=-k_{22}$	$k_{11}=k_{12}$	$k_{21}=-k_{22}$
2.1	0.0626	-0.170	1.201	0.105
2.5	0.260	-0.101	1.196	0.171
3	0.395	-0.0644	1.196	0.202
4	0.574	-0.0175	1.180	0.180
6	0.768	0.0274	1.110	0.109
10	0.906	0.0361	1.046	0.0567
$\infty$	1.0	0	1.0	0

from the x-axis (for the notation see the inserts in Figures 2 and 3). In Tables 5-9 the normalized stress intensity factors are defined by

$$\begin{aligned} k_{11} &= \frac{k_1(b+a)}{\sigma_0 \sqrt{a}}, & k_{21} &= \frac{k_2(b+a)}{\sigma_0 \sqrt{a}}, \\ k_{12} &= \frac{k_1(b-a)}{\sigma_0 \sqrt{a}}, & k_{22} &= \frac{k_2(b-a)}{\sigma_0 \sqrt{a}}, \end{aligned} \quad (17)$$

i.e., the first subscripts 1 and 2 respectively refer to the first and second mode, and the second subscripts refer to the right and left crack tips. Again in all the results given in Tables 5-9 the material constants are  $\mu_2=0$ , or  $\mu_2=23\mu_1$ ,  $\kappa_1=1.6$ ,  $\kappa_2=1.8$ , and the external load  $\sigma_0$  is perpendicular to the plane of the crack. From Table 5 it is seen that  $k_{11}$  may be greater than 1 for the stiffer inclusion and considerably less than 1 for the hole. This and the similar results observed in the subsequent tables may at first appear to be somewhat paradoxical. However if one considers the distribution of the stresses in an uncracked matrix shown in Figures 2 and 3, the explanation for the trends would be apparent.

Tables 6-9 show some further results for an arbitrarily oriented crack in the neighborhood of an elastic inclusion or a hole. Note that in these examples the shear component of the stress intensity factor  $k_{2j}$ ,

( $j=1,2$ ) is not zero. Thus from (9) it can be shown that at the crack tip  $x=b-a$  (see Figures 2 and 3) the direction of probable crack propagation will be towards the interface if  $\mu_2=0$  (or generally if  $\mu_2 < \mu_1$ ), and away from the interface if  $\mu_2 > \mu_1$ . The details of the arbitrarily oriented crack problem and further results may be found in [19].

Table 6. Stress intensity factors for a crack perpendicular to the external load ( $R=2a$ ,  $b=3a$ ,  $\kappa_1=1.6$ ,  $\kappa_2=1.8$ ).

	$\mu_2 = 0$				$\mu_2 = 23\mu_1$			
c/a	$k_{11}$	$k_{12}$	$k_{21}$	$k_{22}$	$k_{11}$	$k_{12}$	$k_{21}$	$k_{22}$
0		$\rightarrow \infty$	$\rightarrow 0$	$\rightarrow 0$		$\rightarrow 0$	$\rightarrow 0$	$\rightarrow 0$
0.3	1.607	4.267	0.072	-0.391	0.784	0.225	-0.004	0.072
0.5	1.544	3.070	0.113	-0.412	0.792	0.341	-0.006	0.101
1.0	1.430	1.969	0.177	-0.316	0.817	0.613	-0.005	0.057
1.5	1.357	1.552	0.184	-0.241	0.839	0.763	0.008	-0.007
2	1.299	1.337	0.150	-0.243	0.860	0.845	0.034	-0.021
3	1.189	1.083	0.052	-0.282	0.905	0.953	0.089	-0.001
4	1.091	0.957	0.011	-0.261	0.951	1.014	0.117	0.002
8	0.955	0.911	-0.014	-0.114	1.020	1.043	0.088	-0.026
$\infty$	1.0	1.0	0	0	1.0	1.0	0	0

Table 7. Stress intensity factors for a crack perpendicular to the external load ( $R=2a$ ,  $c=a$ ,  $\kappa_1=1.6$ ,  $\kappa_2=1.8$ ).

	$\mu_2 = 0$				$\mu_2 = 23\mu_1$			
b/a	$k_{11}$	$k_{12}$	$k_{21}$	$k_{22}$	$k_{11}$	$k_{12}$	$k_{21}$	$k_{22}$
$\sqrt{3}/2$		$\rightarrow \infty$		$\rightarrow -\infty$		$\rightarrow 0$		$\rightarrow 0$
2.8	1.562	2.700	0.206	-0.790	0.781	0.483	0.002	0.167
3.0	1.430	1.970	0.177	-0.316	0.817	0.613	-0.005	0.057
3.5	1.274	1.548	0.134	-0.047	0.878	0.752	-0.012	-0.047
4	1.193	1.364	0.107	0.023	0.914	0.833	-0.012	-0.068
6	1.070	1.109	0.048	0.032	0.970	0.952	-0.006	-0.041
8	1.036	1.049	0.025	0.015	0.985	0.980	-0.002	-0.021
10	1.022	1.028	0.014	0.007	0.991	0.989	-0.0004	-0.012
$\infty$	1.0	1.0	0	0	1.0	1.0	0	0

Table 8. Stress intensity factors for a crack perpendicular to the external load ( $R = 2a$ ,  $c = 2.2a$ ,  $\kappa_1 = 1.6$ ,  $\kappa_2 = 1.8$ ).

	$\mu_2 = 0$				$\mu_2 = 23\mu_1$			
b/a	$k_{11}$	$k_{12}$	$k_{21}$	$k_{22}$	$k_{11}$	$k_{12}$	$k_{21}$	$k_{22}$
0	0.146	0.146	-0.113	0.113	1.199	1.199	0.127	-0.127
0.5	0.549	0.008	-0.124	-0.101	1.096	1.214	0.202	-0.026
1.0	0.952	0.196	-0.043	-0.372	0.972	1.156	0.212	0.031
2	1.315	0.926	0.092	-0.526	0.847	0.994	0.122	0.035
4	1.188	1.268	0.123	-0.060	0.911	0.871	0.011	-0.066
6	1.084	1.126	0.0765	0.025	0.961	0.941	-0.0016	-0.060

Table 9. Stress intensity factors for a crack perpendicular to the external load ( $c=R$ ,  $b-a=0.2R$ ;  $a$  = constant,  $R$  variable, or  $R$  = constant,  $a$  variable,  $\kappa_1 = 1.6$ ,  $\kappa_2 = 1.8$ ).

	$\mu_2 = 0$				$\mu_2 = 23\mu_1$			
R/a	$k_{11}$	$k_{12}$	$k_{21}$	$k_{22}$	$k_{11}$	$k_{12}$	$k_{21}$	$k_{22}$
5	0.366	0.058	-0.102	-0.021	1.120	1.096	0.0256	0.124
3	0.882	0.257	-0.0774	-0.349	0.984	1.063	0.139	0.150
2	1.247	0.600	0.0935	-0.826	0.868	1.022	0.172	0.162
1.5	1.354	0.926	0.246	-1.226	0.829	0.990	0.168	0.162
1.0	1.312	1.384	0.400	-1.719	0.839	0.951	0.165	0.153
0.75	1.225	1.679	0.453	-1.972	0.866	0.929	0.176	0.144
0.5	1.092	2.180	0.486	-2.239	0.899	0.909	0.194	0.129

(c) The Anti-Plane Shear Problem for Arbitrarily Located Crack

Similar results for the anti-plane shear problem are shown in Figures 4-9 (for the geometry and notation see the inserts in the figures and note that in these figures  $b$  is the distance from the inner crack tip to the center of the inclusion).  $k(+a)$  shown in Figures 4-6 are defined by

$$k(a)p_0\sqrt{a} = k_3(a) = \lim_{x \rightarrow a} \sqrt{2(x-a)} \tau_{lyz}(x,c),$$

$$k(-a)p_0\sqrt{a} = k_3(-a) = \lim_{x \rightarrow -a} \sqrt{2(x+a)} \tau_{lyz}(x,c), \quad (18)$$

and in Figure 7 we have

$$k(\bar{+}a) = k_3(\bar{+}a)/(p_0\sqrt{R}) , \quad (19)$$

where  $p_0 = \tau_{1yz}$ ,  $y \rightarrow \bar{+}\infty$ , is the external load. In Figure 7 the asymptotic slopes for  $(a/R) \rightarrow 0$  are 0.57, 1.0, and 1.47 for  $m=0$ ,  $m=1$ , and  $m=23.3$ , respectively, where  $m = \mu_2/\mu_1$ . These numbers are obtained from the solution of an infinite plane with a central crack subjected to crack surface tractions  $\tau_{yz}$  given by Figures 8 and 9 at the appropriate locations (which give the stresses in the uncracked matrix containing an elastic inclusion or a hole). The details of the anti-plane problem may be found in [20].

As mentioned earlier, the general three-dimensional matrix-inclusion-crack problems seem to be analytically intractable. However, under certain simplifying assumptions, the elasticity solutions for a group of three-dimensional problems can be obtained. As an example we may mention the problem of an elastic matrix containing a penny-shaped crack and reinforced by elastic filaments which are distributed perpendicular to and around the crack. The solution of this problem is given in [21]. Some sample results taken from [21] may be found in [22].

#### REFERENCES

1. Erdogan, F. (1969), in "Fracture", Vol. 2, Chapter 5, H. Liebowitz, ed., Academic Press.
2. Irwin, G.R. (1948), in "Fracturing of Metals", ASM, Cleveland, Ohio.
3. Orowan, E. (1952), in "Proceedings of the Symposium on Fatigue and Fracture of Metals", Wiley, New York.
4. Eshelby, J.D. (1951), Phil. Trans. Roy. Soc. London, Ser. A 244, 87-112.
5. Cherepanov, G.P. (1967), Appl. Math. Mech. (PMM), 31, 503-512.
6. Rice, J.R. (1968), J. Appl. Mech., 35, 379-386.
7. Malyshev, B.M. and Salganik, R.L. (1965), Int. J. Fracture Mechanics, 1, 114-128.
8. Wells, A.A. (1971), Proc. 3rd Canadian Conf. Appl. Mech. (CANCAM).

9. Fearneough, G.D. and Watkins, B. (1968), Int. J. Fracture Mechanics, 4, 233.
10. Erdogan, F. and Ratwani, M. (1971), Nuclear Engng. and Design, 20, 265-286.
11. Erdogan, F. and Ratwani, M. (1972), Int. J. Fracture Mechanics, 8, 413-426.
12. Cook, T.S. and Erdogan, F. (1972), Int. J. Engng. Sci., 10, 667-697.
13. Erdogan, F. and Sih, G.C. (1963), J. Basic Engng., Trans. ASME, 85, Series D., 519-525.
14. Erdogan, F. and Biricikoglu, V. (1973), Int. J. Engng. Sci. (to appear).
15. Isida, M. (1970), J. Engng. Fracture Mechanics, 2, 61-79.
16. Atkinson, C. (1972), Int. J. Engng. Sci., 10, 127-136.
17. Bhargava, R.D. and Bhargava, R.R. (1973), Int. J. Engng. Sci., 11, 437-449.
18. Erdogan, F. and Gupta, G.D. (1973), NASA Project Report NGR-39-007-011, Lehigh University.
19. Erdogan, F., Gupta, G.D. and Ratwani, M. (1973), NASA Project Report NGR-39-007-011, Lehigh University.
20. Chan, K. (1972), "The Anti Plane Shear Problem for a Crack Near an Elastic Inclusion", M.S. Thesis, Lehigh University.
21. Pacella, A.H. (1970), "A Penny-Shaped Crack in a Filament-Reinforced Matrix", Ph.D. Dissertation, Lehigh University.
22. Erdogan, F. (1972), J. Engng. Fracture Mechanics, 4, 811-840.

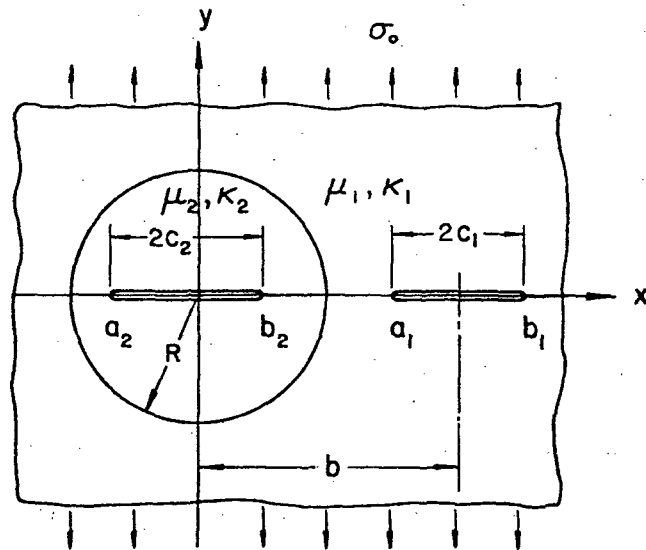


Figure 1. Geometry of radial cracks.

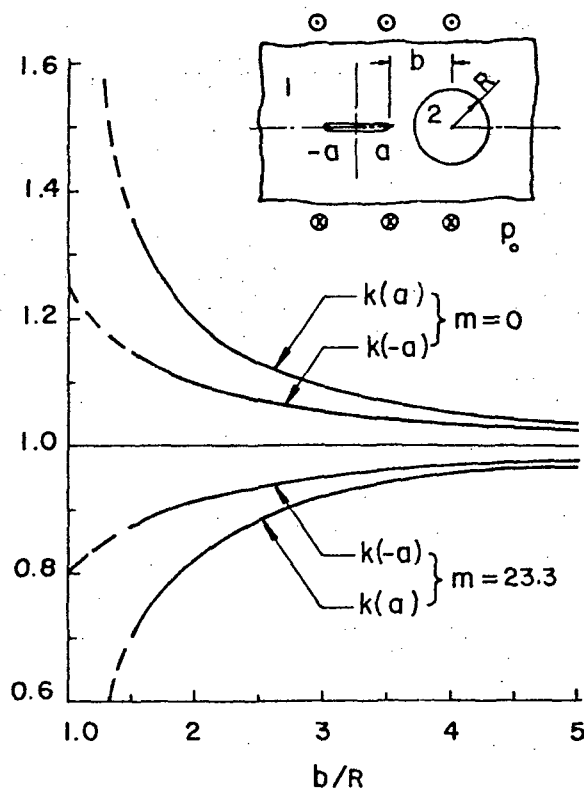


Figure 4. Stress intensity factors for the antiplane shear problem ( $k = k_3 / p_0 \sqrt{a}$ ,  $R = a$ ).

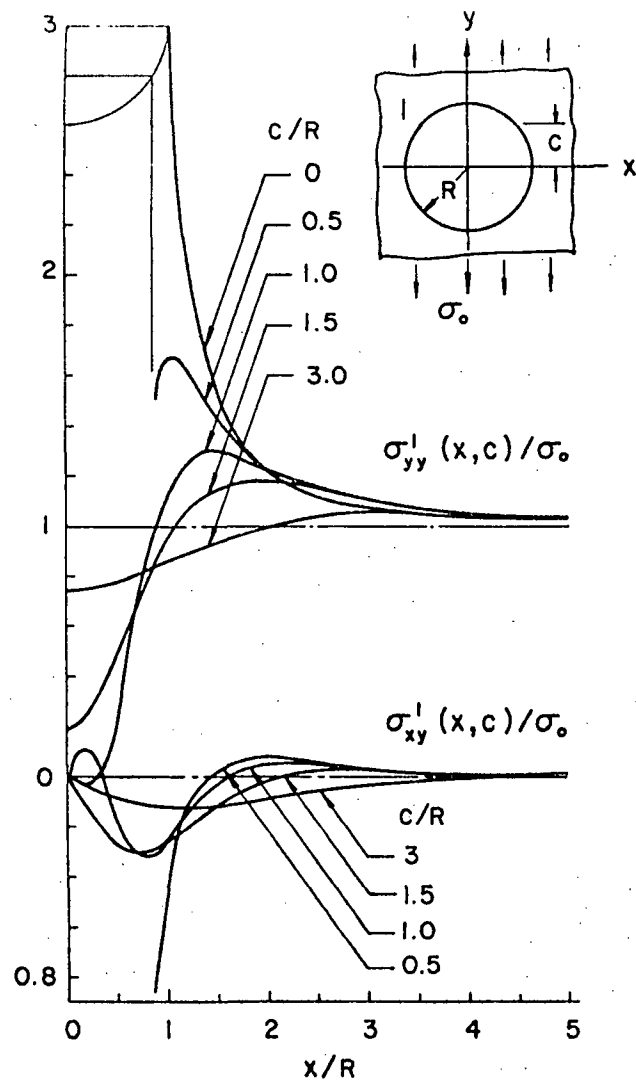


Figure 2. Stresses in an elastic matrix with a hole.

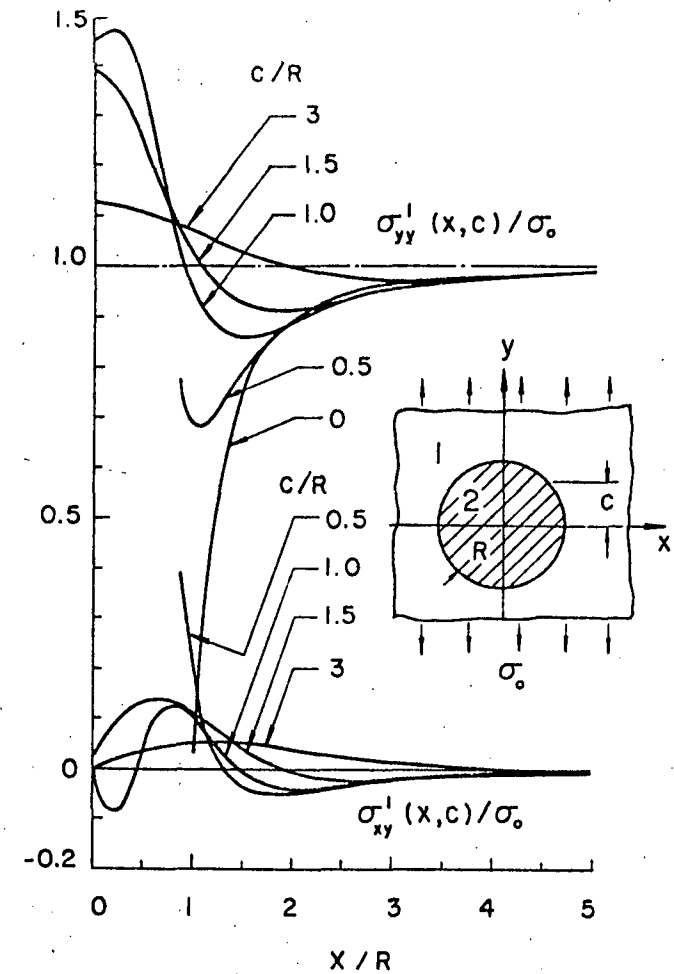


Figure 3. Stresses in an elastic matrix with an inclusion ( $\mu_2 = 23\mu_1$ ,  $\kappa_1 = 1.6$ ,  $\kappa_2 = 1.8$ ).

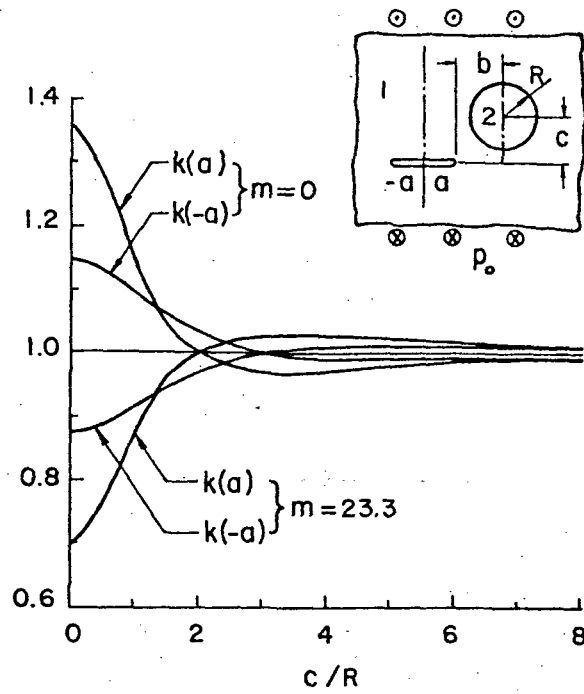


Figure 5. Stress intensity factors for the antiplane shear problem ( $k = k_3/p_0\sqrt{a}$ ,  $R = a$ ,  $b = 1.5R$ ).

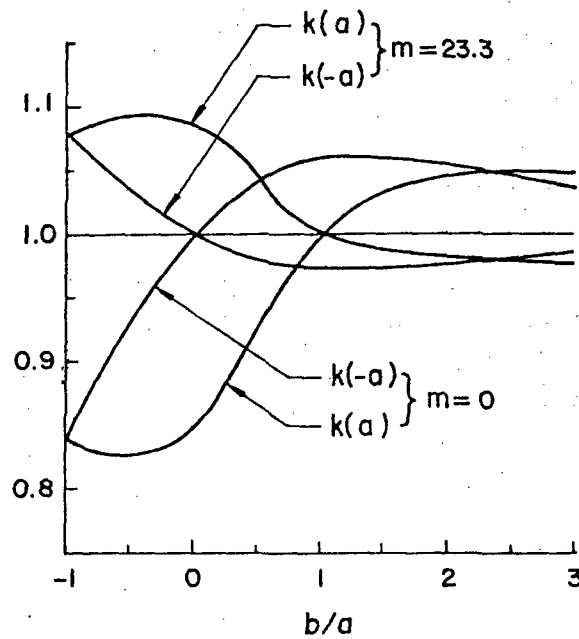


Figure 6. Stress intensity factors for the antiplane shear problem ( $k = k_3/p_0\sqrt{a}$ ,  $R = a$ ,  $c = 1.5R$ ).

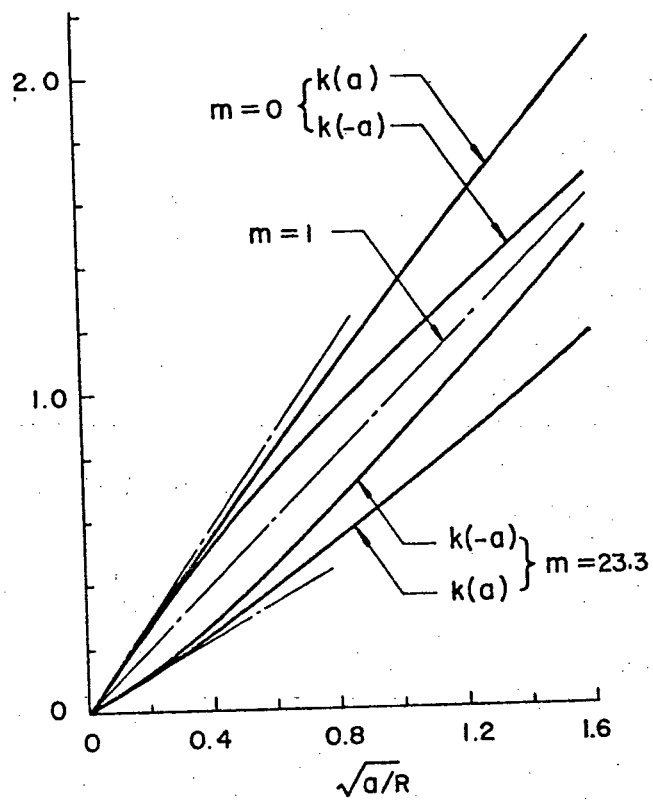


Figure 7. Stress intensity factors for the antiplane shear problem ( $k = k_3/p_0\sqrt{R}$ ,  $c = 0$ ,  $b = 1.5R$ ).

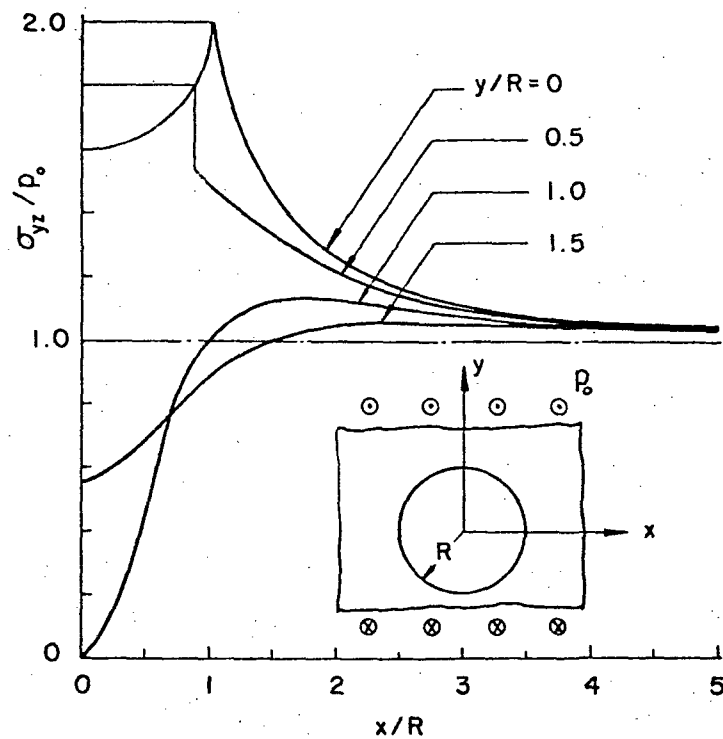


Figure 8. The shear stress  $\tau_{yz}$  in a matrix with a circular hole.

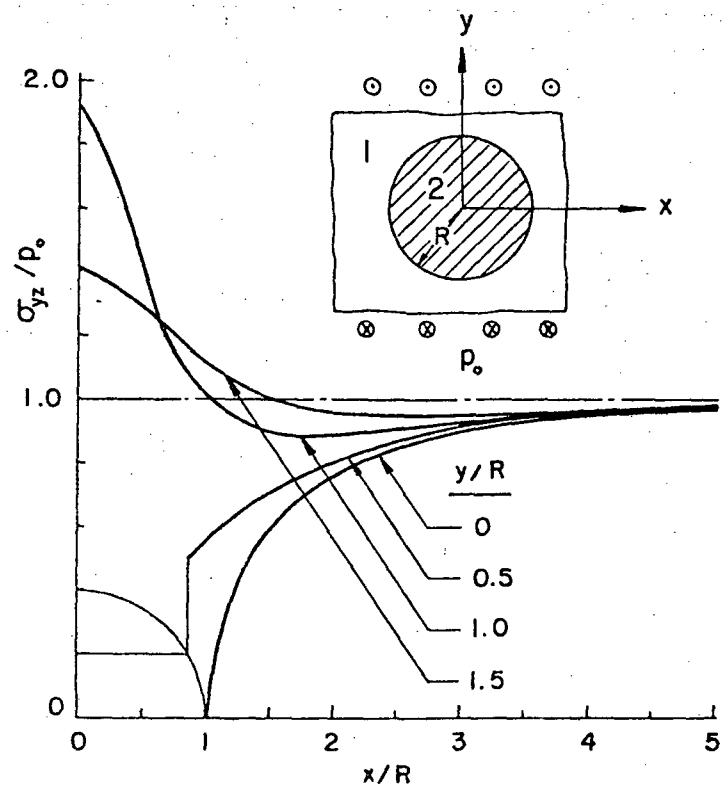


Figure 9. The shear stress  $\tau_{yz}$  in a matrix with a circular inclusion ( $\mu_2 = 23.3 \mu_1$ ).